Desalination and Water Treatment
www.deswater.com
doi: 10.1080/19443994.2014.986766

57 (2016) 3619–3631
February

Taylor & Francis
Taylor & Francis Group

Adsorptive removal of Ni^{2+} and Cd^{2+} by polymethacrylamide and polyvinylamine derivatives from water

Atul Kumar Kushwaha[a,b,*], Neha Gupta[b], M.C. Chattopadhyaya[b]

[a]*Department of Chemistry, Sri Sai University, Palampur, Himachal Pradesh, India, email: atulkk2008@gmail.com (A.K. Kushwaha)*
[b]*Department of Chemistry, University of Allahabad, Allahabad, Uttar Pradesh 211002, India, emails: neha.evs07@gmail.com (N. Gupta), mcc46@rediffmail.com (M.C. Chattopadhyaya)*

Received 2 December 2013; Accepted 7 November 2014

ABSTRACT

Heavy metals are environmental toxins entering in the food chain through drinking water causing serious health hazards. In the present work, surface of polymethyl methacrylate and polyvinyl chloride was functionalized with amine groups using 1,2-ethylenediamine and characterized by Fourier transform infrared spectroscopy, scanning electron microscopy, and elemental analysis. The resulting polymers polymethacrylamide derivative of 1,2-ethylenediamine (PMAm) and polyvinylamine derivative of 1,2-ethylenediamine (PVAm) were tested for the adsorption of Ni^{2+} and Cd^{2+} ions from water. Effect of various physico-chemical parameters such as pH, adsorbent dose, contact time, initial Ni^{2+} and Cd^{2+} ion concentration, and temperature on adsorption of Ni^{2+} and Cd^{2+} ion was investigated. Langmuir and Freundlich isotherm models were used to analyze equilibrium data of adsorption. Monolayer adsorption capacity of PMAm-Ni^{2+}, PMAm-Cd^{2+}, PVAm-Ni^{2+} and PVAm-Cd^{2+} systems was found to be 7.87 mg/g, 10.57 mg/g, 23.92 mg/g, and 31.44 mg/g, respectively. Kinetic studies were performed using pseudo-first-order, pseudo-second-order kinetic models, and intraparticle diffusion method. The spontaneity and nature of adsorption process were determined by thermodynamic parameters, such as change in Gibb's free energy (ΔG°), enthalpy (ΔH°), and entropy (ΔS°).

Keywords: Adsorption; Nickel; Cadmium; Isotherm; Kinetics; Thermodynamics

---

1. Introduction

Industrialization and urbanization in the world have led to an increase in pollutants concentration in water bodies creating serious ecological problems. Heavy metals can be distinguished from other toxic pollutants, since they are not biodegradable and can be accumulated in living tissues, causing various diseases and disorders. Nickel and cadmium are the elements of great concern from a toxicity point of view. The maximum admissible concentration set by WHO for nickel and cadmium in drinking water are 0.02 and 0.003 mg/L, respectively. Nickel compounds can cause a variety of adverse effects, such as skin dermatitis, lung fibrosis, cardiovascular diseases, gastrointestinal distress, kidney problems, and cancer of the respiratory tract [1]. Cadmium is a toxic metal causing both acute and chronic toxicity in humans. Intake of cadmium may cause acute gastrointestinal problems, such as vomiting and diarrhea, while chronic exposure to cadmium for a long time may cause kidney

---

*Corresponding author.

damage, reproductive problems, bone damage, and cancer [2].

Surface modification of synthetic polymer with selective ligands makes it a promising adsorbent for metal removal from aqueous solutions, because of its good mechanical strength, high selectivity, stability, and sensitivity to the low concentration of ions [3]. Several polymers and their composites have been tried by various researchers for adsorptive removal of heavy metals from aqueous solution. Liu et al. [4] reported the selective removal of copper and lead ions from aqueous solutions by diethylenetriamine (DETA)-functionalized polymeric adsorbent. Vasudevan et al. [5] reported pore-functionalized polymer membranes for preconcentration of heavy metal ions. Nastasovic et al. [6] reported chromium sorption on amino-functionalized macroporous glycidyl methacrylate copolymer. Zhao et al. [7] reported ethylenediamine (EDA)-functionalized magnetic polymers (EDA-MPs) for removal of Cr (VI). Kiani et al. [8] reported adsorption of Hg(II), Fe (III), Pb(II), Ag(I), and Zn(II) from aqueous solutions utilizing functionalized polyacrylonitrile sorbents. Sayari [9] reported adsorption of copper on amine-functionalized SBA-15.

Polymethyl methacrylate (PMMA) is a transparent thermoplastic and synthetic polymer of methyl methacrylate. It is a low-cost material used for several purposes, such as in medical, optics, semiconductor, paints, etc. Polyvinyl chloride (PVC) is a thermoplastic polymer. It is a vinyl polymer constructed of repeating vinyl groups (ethenyls) having one hydrogen replaced by chloride. Polyvinyl chloride is the third most widely produced plastic, after polyethylene and polypropylene. PVC is widely used in construction because it is cheap, durable, and easy to assemble. Nowadays, most adsorbents developed for the removal of heavy metal ions rely on their interactions with the functional groups on the surfaces of the adsorbents, and hence, the functional groups have important effects on the effectiveness, capacity, and reusability of the adsorbents.

The aim of present work is to functionalize the surface of PMMA and PVC with amine functional groups in order to get active adsorption sites on its surface, and to test the resulting materials [polymethacrylamide derivative of 1,2-ethylenediamine (PMAm) and polyvinylamine derivative of 1,2-ethylenediamine (PVAm)] for the removal of Ni^{2+} and Cd^{2+} from water by batch adsorption method.

2. Materials and methods

2.1. Synthesis of PMAm and PVAm

PMMA was obtained from Sigma-Aldrich, India and 1,2-ethylenediamine was obtained from Merck. Five grams PMMA was dissolved in 50 mL of toluene followed by addition of 50 mmol of 1,2-ethylenediamine. Resulting mixture was stirred for 8 h at 90˚C. After cooling the reaction mixture, microsolids of poly-methyl methacrylamide derivative of 1,2-ethylenediamine (PMAm) comes out of solution. The final material (PMAm) (Fig. 1(a)) was dried and kept in desiccator for its use as an adsorbent.

Polyvinyl chloride (PVC) and 1,2-ethylenediamine were obtained from Merck. Potassium t-butoxide (t-BuOK) (2.5 mM) and tetra-n-butylammonium bromide (n-Bu4NBr) (0.1 mM) were added to a cooled solution (0˚C) of 1,2-ethylenediamine (2.0 mM) in dimethylformamide (DMF) (5 mL) and the resulting reaction mixture was stirred at 0˚C for 15 min. After that PVC (2.0 mM) was added and resulting reaction mixture was left for stirring (10 h) at room temperature. The mixture was concentrated in vacuum, and ice water was added in concentrated mixture and filtered. The final compound, poly-vinylamine derivative of 1,2-ethylenediamine (PVAm) (Fig. 1(b)) was dried and kept in desiccator for its use as an adsorbent.

2.2. Adsorption experiments

Stock solution (1,000 mg/L) of each metal ion was prepared by dissolving required amount of nitrate salt of metal ($Ni(NO_3)_2{\cdot}6H_2O$ and $Cd(NO_3)_2{\cdot}4H_2O$ obtained from Merck) into double-distilled water. The experimental solution of desired concentration was prepared by successive dilution of stock solution. The initial pH of each metal ion solution was maintained by adding 0.1 M HNO_3 or 0.1 M NaOH. The batch experiments were performed in 150 mL of conical flask by adding preweighed amount of adsorbent in 50 mL of metal ion solution. The mixture was stirred on magnetic stirrer (Remi) at the speed of 200 rpm. The adsorption was monitored by determining the concentration of metal ion in solution by atomic absorption spectrophotometer (ECIL-4141).

Percentage removal of metal ion and quantity of metal ion adsorbed on adsorbent at the equilibrium time (q_e) was calculated using Eqs. (1) and (2) respectively.

$$\%\ \text{removal} = 100 \times (C_0 - C_e)/C_0 \tag{1}$$

$$q_e = (C_0 - C_e)V/M \tag{2}$$

where C_0 and C_e are the initial and the equilibrium concentrations (mg/L) of metal ion in solution, respectively. q_e is the quantity of metal ion adsorbed on the adsorbent at the time of equilibrium (mg/g), V is the

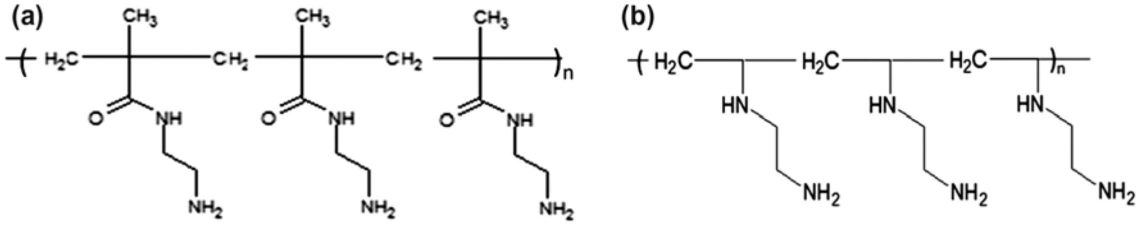

Fig. 1. Chemical structure of PMAm (a) and PVAm (b).

volume (L) of solution and *M* is the mass of adsorbent (g) taken for experiment.

Batch experiments were carried out to determine the effects of pH, adsorbent dose, initial metal ion concentration, contact time, and temperature on adsorption by varying the parameter under study and keeping other parameters constant. All adsorption experiments were performed in triplicate and the mean values were used in data analysis.

3. Results and discussion

3.1. Characterization of PMAm and PVAm

The FTIR spectra of PMAm and PVAm were recorded on FTLA2000 spectrophotometer using KBr disk method in the range of 4,000–500 cm^{-1} (Fig. 2(a) and (b)). Spectrum of PMAm showed a band around 3,500 cm^{-1} was due to stretching of N–H group. The bands at 2,996 and 2,951 cm^{-1} were due to C–H stretching and the corresponding bending peak occurred at 1,435 cm^{-1}. The band at 1,730 cm^{-1} was due to C=O stretching in PMAm. Spectrum of PVAm showed a band around 3,500 cm^{-1} was due to stretching of N–H group. The bands at 2,996 and 2,951 cm^{-1} were due to C–H stretching and the corresponding bending peak occurred at 1,435 cm^{-1}. The band at 1,730 cm^{-1} was due to N–H bending in PVAm. SEM micrograph (Fig. 3(a) and (b)) revealed the surface morphology of the PMAm and PVAm, respectively, which was investigated by SUPRA 40VP scanning electron microscope operated at 10 kV accelerating voltage. The surface of polymer was homogenous, porous, and rough in nature, which provides the suitable binding sites for adsorption of metal ions. Elemental analysis of PMAm and PVAm was done by Elementar Vario EL III. The wt% of C, H, N, and O in PMAm was 56.52, 21.35, 13.12, and 9.01%, respectively, and the wt% C, H, and N in PVAm was 56.32, 32.15, and 11.53%, respectively. This was very close to calculated value of wt% of elements.

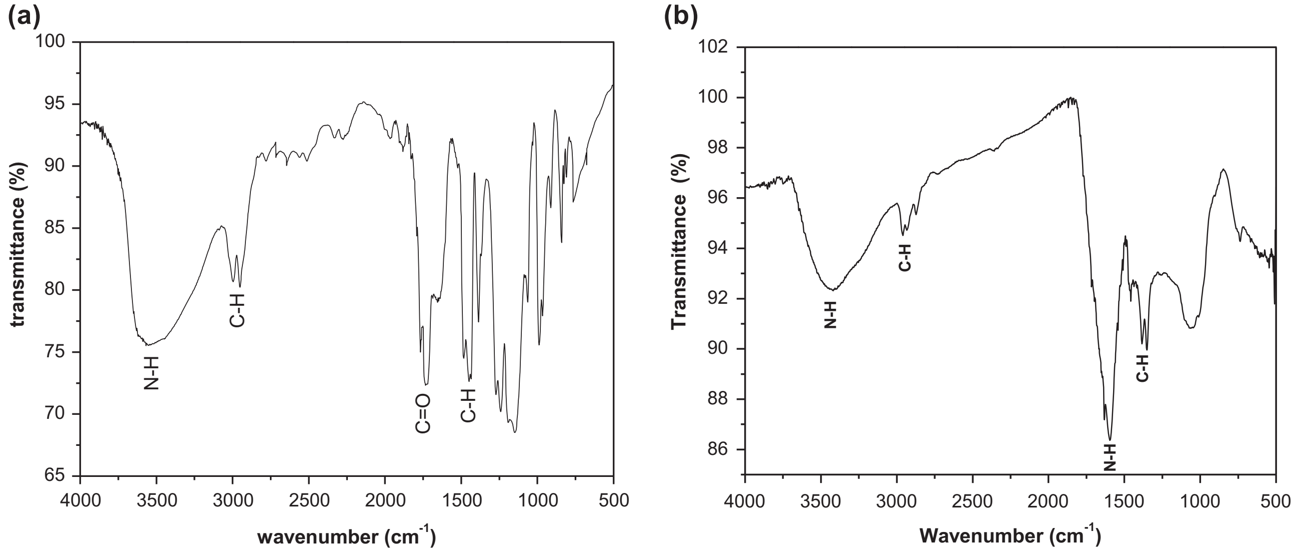

Fig. 2. FTIR spectrum of PMAm (a) and PVAm (b).

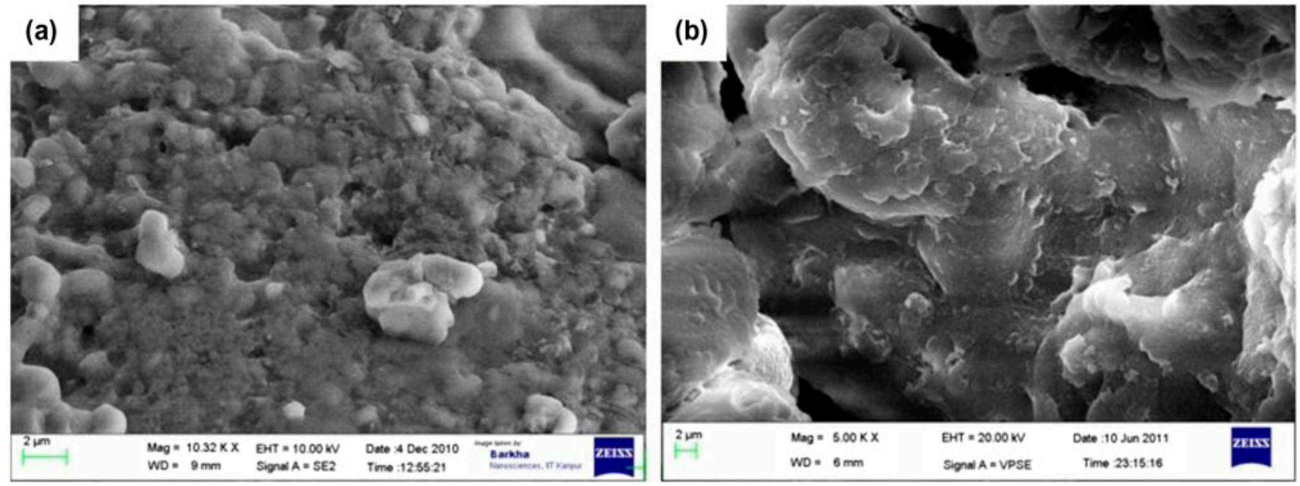

Fig. 3. SEM image of PMAm (a) and PVAm (b).

3.2. Effect of pH

The pH is one of the most important factors controlling the adsorption of metal ion onto PMAm and PVAm. The influence of pH on removal of Ni^{2+} and Cd^{2+} by PMAm and PVAm was studied over the pH range 2–6. Fig. 4 showed that the adsorption was increased from 9 to 48%, 15 to 65%, 18 to 65%, and 31 to 96% for the PMAm-Ni^{2+}, PMAm-Cd^{2+}, PVAm-Ni^{2+}, and PVAm-Cd^{2+} systems, respectively, with increasing pH from 2 to 6. At lower pH values, hydrogen ion competes with metal ions which reduce the adsorption of metal ion. At higher pH values, there is reduced competition between hydrogen ion and metal ion, which enhance the adsorption capacity of adsorbent for metal ion. Further increase in pH may cause precipitation of metal ions due to formation of hydroxide [10]. Therefore, the pH value higher than six was avoided for further experiments.

3.3. Effect of adsorbent dose

The effect of adsorbent dose on removal of Ni^{2+} and Cd^{2+} was studied using adsorbent dose in the range of 0.5–3 g/L for 10 mg/L of initial metal ion

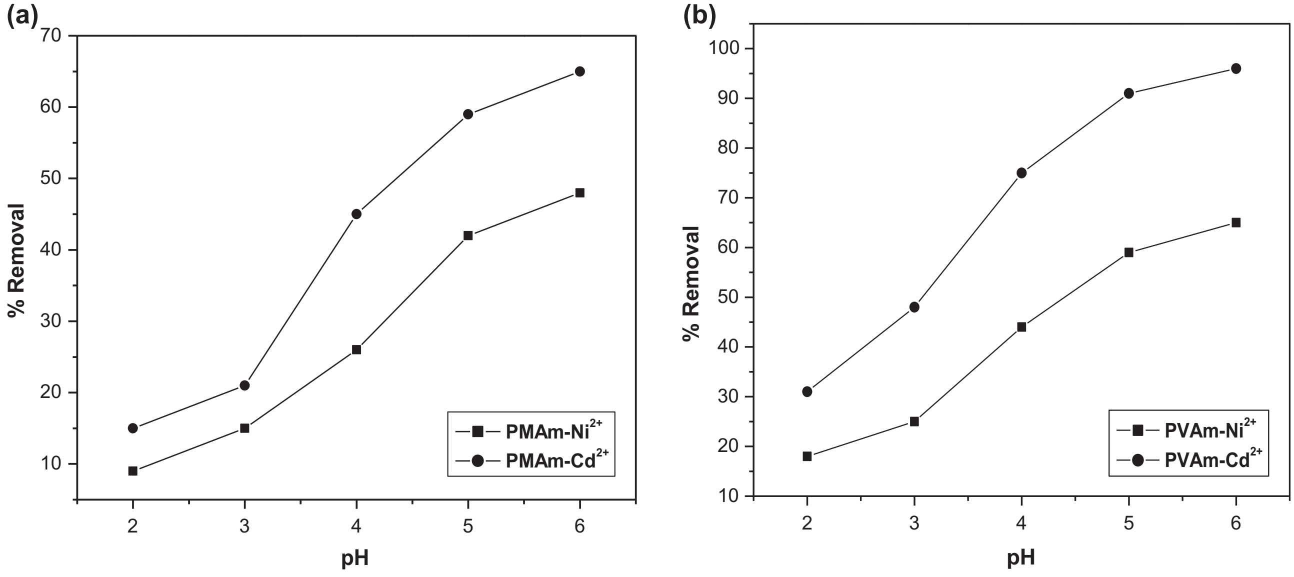

Fig. 4. Effect of pH on removal of Ni^{2+} and Cd^{2+} by PMAm (a) and PVAm (b).

concentration. Fig. 5 shows that on increasing adsorbent dose from 0.5 to 2 g/L, the adsorption increased from 10 to 48%, 25 to 65%, 32 to 65%, and 52 to 96% for the PMAm-Ni^{2+}, PMAm-Cd^{2+}, PVAm-Ni^{2+}, and PVAm-Cd^{2+} systems, respectively. Such a trend is mainly attributed to an increase in the adsorptive surface area and the availability of more adsorption sites [11]. There was no significant change observed as the adsorbent dose was further increased. This was due to the concentration of metal ions reached at equilibrium status between solid and solution phases.

3.4. Effect of initial metal ion concentration

To observe the effect of initial metal ion concentration on removal of metal ion, the experiments were conducted over the range of 5–25 mg/L for PMAm and 10–50 mg/L for PVAm for each metal ion (Fig. 6). It was observed that the % removal decreased from 56 to 38% and from 71 to 52.4% for the PMAm-Ni^{2+} and PMAm-Cd^{2+} systems, respectively, as the initial metal ion concentration increased from 5 to 25 mg/L. The % removal decreased from 65 to 50.2% and 96 to 89.4% for the PVAm-Ni^{2+} and PVAm-Cd^{2+} systems, respectively, as the initial metal ion concentration increased from 10 to 50 mg/L.

3.5. Effect of contact time

Fig. 7 showed the effect of contact time on removal of metal ions (Ni^{2+} and Cd^{2+}) by PMAm and PVAm. It can be seen that the adsorption rate of metal ions was rapid in the initial stages and was gradually decreased with the progress of adsorption, until the equilibrium reached. The equilibrium time was 30 min for PMAm-Ni^{2+} and PMAm-Cd^{2+} systems and 40 min for PVAm-Ni^{2+} and PVAm-Cd^{2+} systems. As the contact time increased after equilibrium time, no change was observed in adsorption of metal ion.

3.6. Adsorption isotherms

Adsorption isotherm describes the nature of adsorbate–adsorbent interaction. In the present study, the equilibrium data were analyzed using the Langmuir and Freundlich isotherm models. The analysis of the isotherm data by seeing how well they can be accommodated by different models is an important step in establishing a model that can be successfully used for design purposes.

3.6.1. Langmuir isotherm model

The Langmuir model is valid for monolayer adsorption onto a surface with a finite number of identical sites which are homogeneously distributed over the adsorbent surface. The well-known expression of the Langmuir model [12] is given as:

$$q_e = Q_m b C_e / (1 + b C_e) \tag{3}$$

The linearized forms of Eq. (3) can be written as follows:

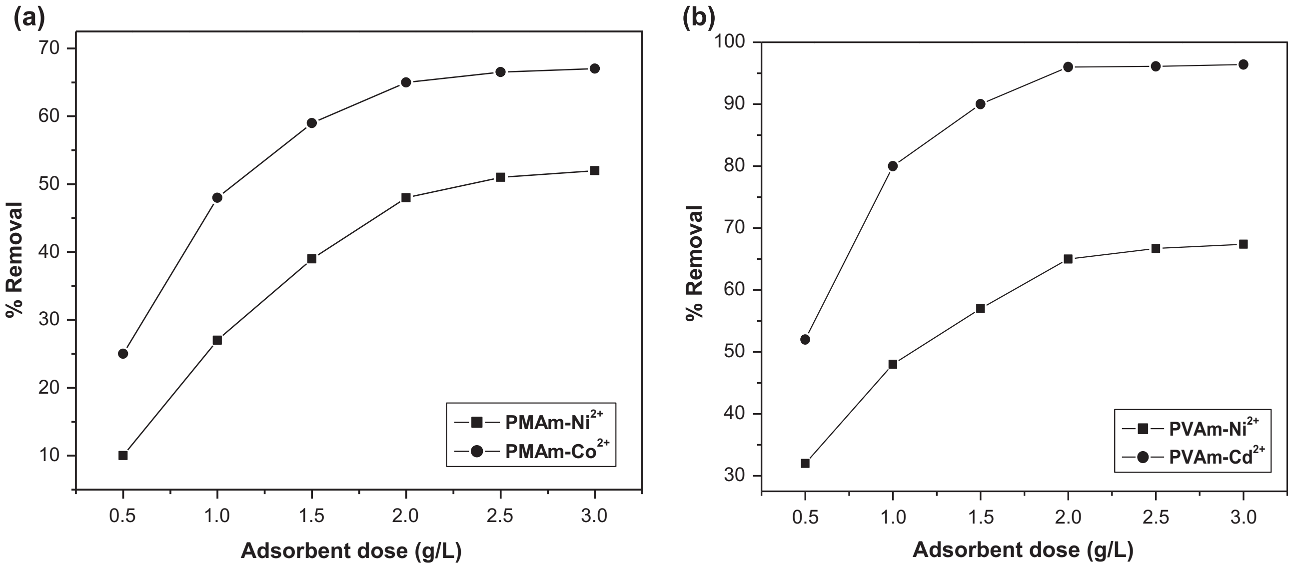

Fig. 5. Effect of adsorbent dose on removal of Ni^{2+} and Cd^{2+} by PMAm (a) and PVAm (b).

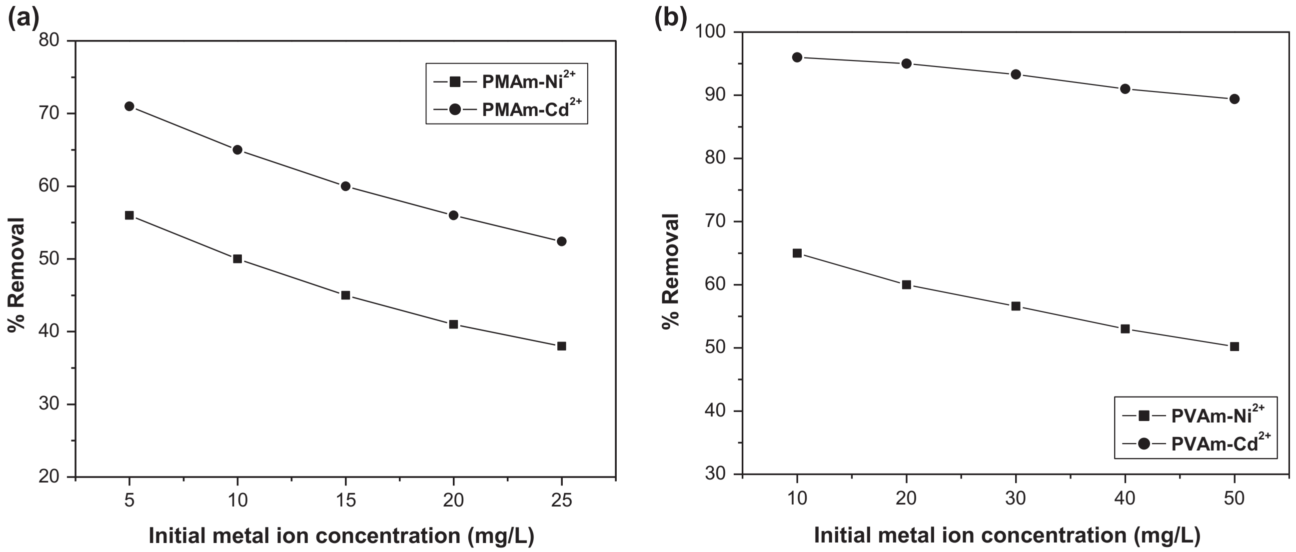

Fig. 6. Effect of initial metal ion concentration on removal of Ni^{2+} and Cd^{2+} by PMAm (a) and PVAm (b).

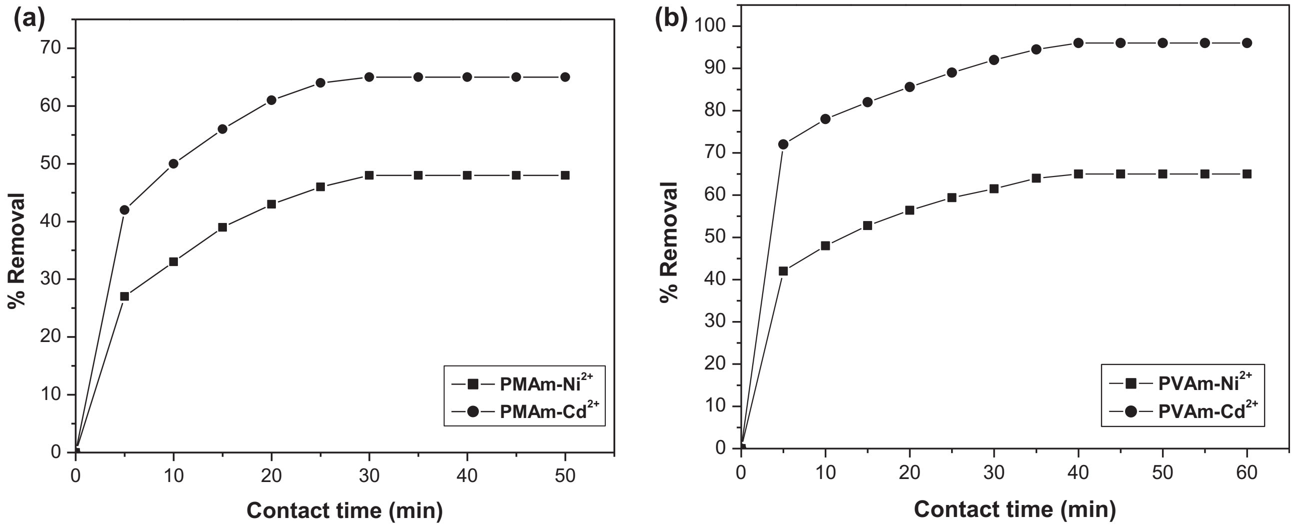

Fig. 7. Effect of contact time on removal of Ni^{2+} and Cd^{2+} by PMAm (a) and PVAm (b).

$$C_e/q_e = 1/bQ_m + C_e/Q_m \tag{4}$$

where q_e is the adsorption density (mg/g) at equilibrium of metal ion, C_e is the equilibrium concentration (mg/L) of the metal ion in solution, Q_m is the monolayer adsorption capacity (mg/g), and b is the Langmuir constant (L/mg) related to the free energy of adsorption. The values of Q_m and b were calculated from the slopes ($1/Q_m$) and intercepts ($1/bQ_m$) of the plots of C_e/q_e vs. C_e (Fig. 8(a)) and are presented in Table 1. Linear plots of C_e/q_e vs. C_e showed that all the four adsorption systems followed the Langmuir isotherm model. Experimental results showed that monolayer adsorption capacity of all the four systems was in the order PMAm-Ni^{2+} < PMAm-Cd^{2+} < PVAm-Ni^{2+} < PVAm-Cd^{2+}. The values of the maximum adsorption capacities for the adsorption of Ni^{2+} and Cd^{2+} ions on different adsorbents used in the literature with adsorbent of the present study are summarized in Table 2 [13–30].

The essential characteristic of the Langmuir isotherm can also be evaluated by dimensionless adsorption intensity, R_L, given by following expression:

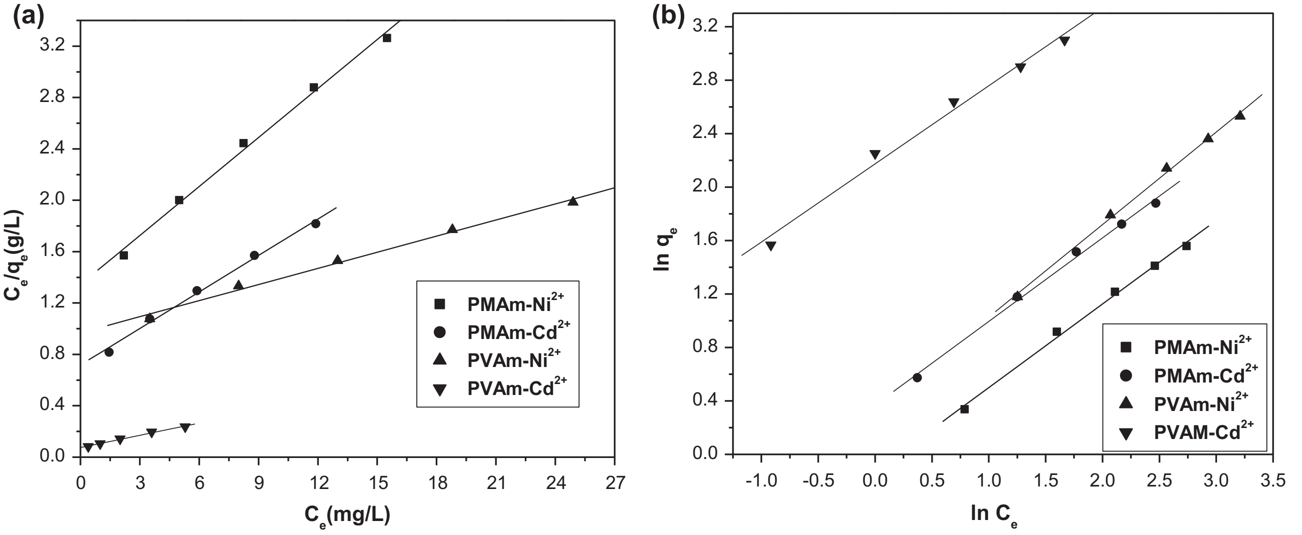

Fig. 8. Langmuir (a) and Freundlich (b) isotherm plots for adsorption of Ni^{2+} and Cd^{2+} on PMAm and PVAm.

Table 1
Isotherm parameters for adsorption of Ni^{2+} and Cd^{2+} ions on PMAm and PVAm

	Langmuir parameters			Isotherm	Freundlich parameters		Isotherm
Adsorption systems	Q_m (mg/g)	b	R_L	R^2	K_f	n	R^2
PMAm-Ni^{2+}	7.87	0.094	0.404	0.994	0.80	1.6	0.995
PMAm-Cd^{2+}	10.57	0.131	0.265	0.993	1.44	1.6	0.996
PVAm-Ni^{2+}	23.92	0.043	0.327	0.992	1.39	1.44	0.997
PVAm-Cd^{2+}	31.44	0.426	0.035	0.991	8.78	1.71	0.988

$$R_L = 1/(1 + bC_0) \tag{5}$$

where C_0 (mg/L) is the highest initial concentration of metal ion and b (L/mg) is the Langmuir constant. The parameter R_L indicates the shape of the isotherm to be either unfavorable ($R_L > 1$), linear ($R_L = 1$), favorable ($0 < R_L < 1$), or irreversible ($R_L = 0$). In our experiments the values of

R_L for PMAm-Ni^{2+}, PMAm-Cd^{2+}, PVAm-Ni^{2+}, and PVAm-Cd^{2+} systems were in between 0 and 1 (Table 1), suggesting that the adsorption of Ni^{2+} and Cd^{2+} on the surface of PMAm and PVAm was favorable. In addition, the lower R_L value for PVAm-Cd^{2+} (< 0.04) implied that the interaction of Cd^{2+} ions with PVAm might be relatively strong.

3.6.2. Freundlich isotherm model

The Freundlich model [31] is an empirical equation based on adsorption onto a heterogeneous surface is given below by Eq. (6)

$$q_e = K_f C_e^{1/n} \tag{6}$$

The logarithmic forms of Eq. (6) can be written as follows:

$$\ln q_e = \ln K_f + (1/n) \ln C_e \tag{7}$$

where K_f and n are Freundlich constants related to adsorption capacity [mg/g (mg/L)$^{-1/n}$] and adsorption intensity of adsorbents. The values of the K_f and n were calculated from the intercepts (ln K_f) and slopes ($1/n$) of the plots ln q_e vs. ln C_e (Fig. 8(b)) and are presented in Table 1. Linear plots of ln q_e vs. ln C_e showed that the adsorption isotherm of Ni^{2+} and Cd^{2+} on PMAm and PVAm also fitted well in the Freundlich isotherm model, and the K_f values showed that the adsorption capacity of PMAm and PVAm was higher for Cd^{2+} than Ni^{2+}. The values of $n > 1$ indicated favorable adsorption conditions [32,33].

Table 2
Comparison of adsorption capacities of various adsorbents for Ni^{2+} and Cd^{2+} ions

Adsorbents	Metal ion	Q_m	References
Bagasse fly ash	Ni^{2+}	6.48	[13]
Calcined Bofe bentonite clay	Ni^{2+}	3.07	[14]
Natural clinoptilolite	Ni^{2+}	4.48	[15]
Pomegranate peel	Ni^{2+}	52.2	[16]
Clinoptilolite	Ni^{2+}	3.28	[17]
Protonated rice bran	Ni^{2+}	46.51	[18]
Activated carbon	Ni^{2+}	44.1	[19]
Waste tea	Ni^{2+}	18.42	[20]
Cashew nut shell	Ni^{2+}	18.86	[21]
Nanocrystalline calcium hydroxyapatite	Ni^{2+}	46.17	[22]
PMAm-Ni^{2+}	Ni^{2+}	7.87	This work
PVAm-Ni^{2+}	Ni^{2+}	23.92	This work
Bagasse fly ash	Cd^{2+}	6.19	[13]
Indigenous clay	Cd^{2+}	0.50	[23]
Areca	Cd^{2+}	3.73	[24]
Activated carbon derived from bagasse	Cd^{2+}	38.03	[25]
Olive cake	Cd^{2+}	65.35	[26]
Poly[4-(4-vinylbenzyloxy)-2-hydrobenzaldehyde]	Cd^{2+}	0.25	[27]
MnO_2-loaded resin	Cd^{2+}	21.45	[28]
Pinus halepensis sawdust	Cd^{2+}	7.35	[29]
Wheat bran	Cd^{2+}	0.66	[30]
PMAm-Cd^{2+}	Cd^{2+}	10.57	This work
PVAm-Cd^{2+}	Cd^{2+}	31.44	This work

3.7. Adsorption kinetics

To investigate the adsorption kinetics of heavy metals onto the PMAm and PVAm, two kinetic models. (i) A pseudo-first-order kinetic model of Lagergren (ii) a pseudo-second-order kinetic model of Ho, were employed to simulate the experimental data.

The differential rate equation for pseudo-first order can be expressed as [34]:

$$dq_t/dt = k_1(q_e - q_t) \qquad (8)$$

where q_e and q_t are the amount of metal ion adsorbed at equilibrium and at time t (mg/g), respectively, and k_1 (min^{-1}) is rate constant of adsorption. Since $q = 0$ at $t = 0$, the initial rate of adsorption ($h_{0,1}$) can be calculated from Eq. (9) as follows:

$$h_{0,1} = k_1 q_e \qquad (9)$$

Integrating Eq. (8) using the boundary condition, $t = 0$ to $t = t$ and $q = 0$ to $q = q$, gives:

$$\ln\,(q_e - q_t) = \ln q_e - k_1 t \qquad (10)$$

The values of k_1 and q_e^{cal} were calculated from the slopes ($-k_1$) and intercepts ($\ln q_e$) of the plots of $\ln (q_e - q_t)$ vs. t (Fig. 9), respectively, and are presented in Table 3. Table 3 shows a good agreement between experimental and calculated q_e values for adsorption of Ni^{2+} and Cd^{2+} on PMAm. The correlation coefficients for the pseudo-first-order kinetic model for PMAm were 0.981 and 0.964 for Ni^{2+} and Cd^{2+}, respectively, indicated the applicability of the pseudo-first-order equation for the adsorption of Ni^{2+} and Cd^{2+} on PMAm. Although the correlation coefficient values for adsorption of metal ions on PVAm was high, the experimental q_e values did not agree with the calculated ones, obtained from the linear plots. This showed that the adsorption of metal ions on PVAm did not follow pseudo-first-order kinetics. The initial adsorption rates ($h_{0,1}$) for PMAm-Ni^{2+}, PMAm-Cd^{2+}, PVAm-Ni^{2+} and PVAm-Cd^{2+} systems were found to be 0.27 mg/g min, 0.48 mg/g min, 0.26 mg/g min, and 0.30 mg/g min, respectively.

The adsorption kinetics may be described by a pseudo-second-order model can be expressed as [35]:

$$dq_t/dt = k_2(q_e - q_t)^2 \qquad (11)$$

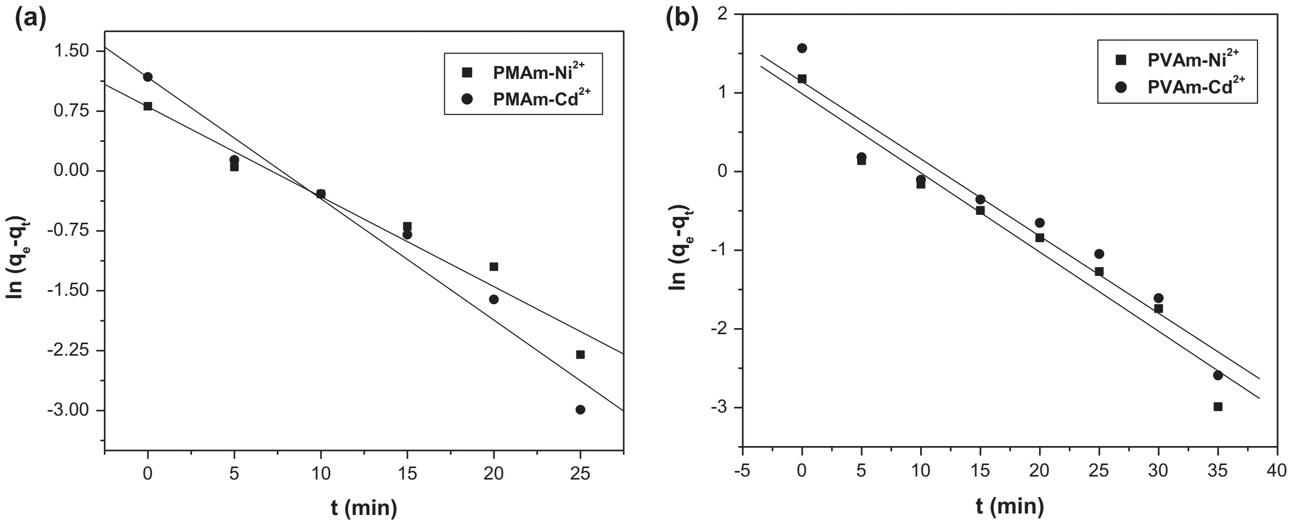

Fig. 9. Pseudo-first-order kinetic plots for adsorption of Ni^{2+} and Cd^{2+} on PMAm (a) and PVAm (b).

Table 3
Kinetic parameters for adsorption of $Ni^{2+}$and Cd^{2+} ions on PMAm and PVAm

		Pseudo-first order				Pseudo-second order					Intraparticle diffusion		
Adsorption systems	q_e^{exp} mg g^{-1}	q_e^{cal}	k_1	$h_{0,1}$	R^2	q_e^{cal}	k_2	$h_{0,2}$	$t_{1/2}$	R^2	k_i	C	R^2
PMAm-Ni^{2+}	2.40	2.35	0.118	0.27	0.981	2.50	0.160	1.00	2.50	0.966	0.334	0.61	0.992
PMAm-Cd^{2+}	3.25	3.22	0.152	0.48	0.964	3.41	0.133	1.54	2.20	0.986	0.369	1.32	0.980
PVAm-Ni^{2+}	3.25	2.68	0.100	0.26	0.949	3.38	0.105	1.19	2.82	0.989	0.286	1.50	0.991
PVAm-Cd^{2+}	4.80	3.12	0.098	0.30	0.935	4.90	0.110	2.64	1.85	0.993	0.289	2.94	0.998

where k_2 is the rate constant of adsorption (g/mg min), q_e and q_t are the amount of metal ion adsorbed (mg/g) at equilibrium and time t (min), respectively. Since $q = 0$ at $t = 0$, the initial rate of adsorption ($h_{0,2}$) can be calculated from Eq. (12) as follows:

$$h_{0,2} = k_2 q_e^2 \tag{12}$$

Integrating Eq. (11) using the boundary condition, $t = 0$ to $t = t$ and $q = 0$ to $q = q$, leads to:

$$t/q_t = 1/k_2 q_e^2 + t/q_e \tag{13}$$

Half-adsorption time ($t_{1/2}$) is the time required for the adsorption to take up half as much metal ion as its equilibrium value. It is an indicator for the adsorption rate. For the pseudo-second order process it can be calculated from the following equation:

$$t_{1/2} = 1/k_2 q_e \tag{14}$$

The values of k_2 and q_e^{cal} were calculated from the intercepts ($1/k_2 q_e^2$) and slopes ($1/q_e$) of the plots of t/q_t vs. t. (Fig. 10), respectively, and are presented in Table 3. Table 3 shows that the correlation coefficient of adsorption of Ni^{2+} and Cd^{2+} on PVAm for the pseudo-second-order kinetic model was 0.989 and 0.993, respectively, and a good agreement between experimental and calculated q_e values indicated the applicability of pseudo-second-order kinetic model for the adsorption of Ni^{2+} and Cd^{2+} on PVAm. The initial adsorption rate ($h_{0,2}$) for PMAm-Ni^{2+}, PMAm-Cd^{2+}, PVAm-Ni^{2+} and PVAm-Cd^{2+} systems were found to be 1.00 mg/g min, 1.54 mg/g min, 1.19 mg/g min, and 2.64 mg/g min, respectively. The half-adsorption time ($t_{1/2}$) for PMAm-Ni^{2+}, PMAm-Cd^{2+}, PVAm-Ni^{2+}, and PVAm-Cd^{2+} systems were found to be 2.5 min, 2.2 min, 2.8, and 1.85 min, respectively.

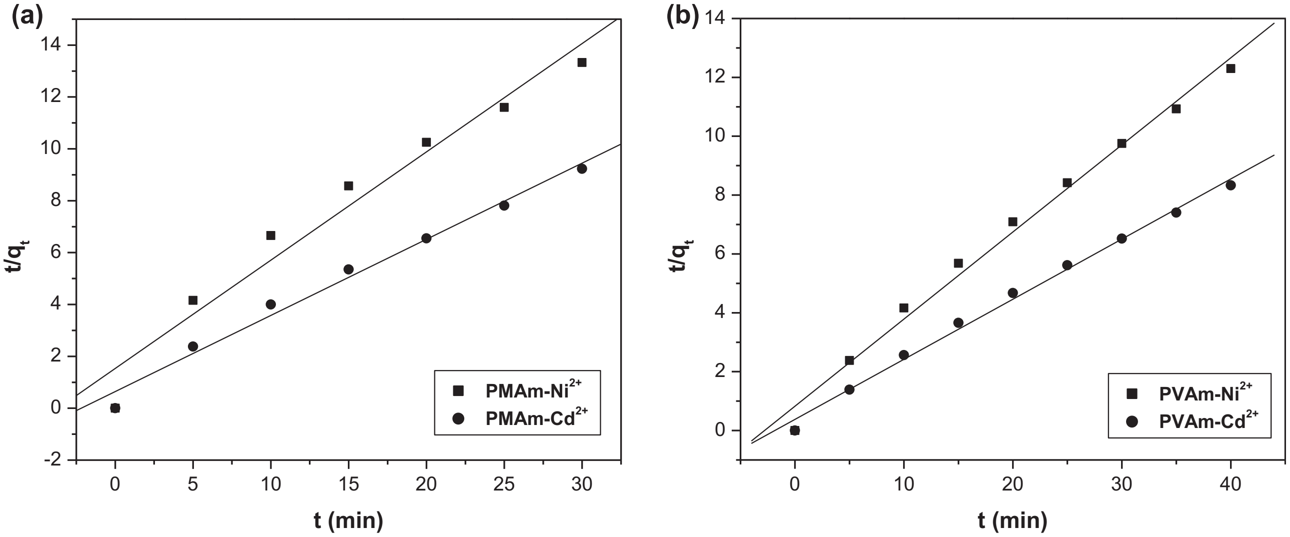

Fig. 10. Pseudo-second-order kinetic plots for adsorption of Ni^{2+} and Cd^{2+} on PMAm (a) and PVAm (b).

3.7.1. Intraparticle diffusion

Adsorption is multi-step process involving the transfer of solute from bulk of solution to surface of adsorbent. Intraparticle diffusion plays an important role in the extent of adsorption and can be expressed as:

$$q_t = k_i t^{0.5} + C \tag{15}$$

where k_i is the intraparticle diffusion constant (mg/g min$^{0.5}$) and the intercept (C) reflects the surface adsorption. The values of k_i were calculated from slopes (k_i) of the plots of q_t vs. $t^{0.5}$ (Fig. 11) and are presented in Table 3. Fig. 11 shows the involvement of two steps in adsorption process, first one representing adsorption of metal ions on the surface of adsorbent and second one described diffusion of metal ions to adsorption site. As shown in table that the rate of diffusion was almost similar for both the metal ions. The value of C was higher for Cd^{2+} than the Ni^{2+} cause difference in % removal.

3.8. Adsorption thermodynamics

To observe the effect of temperature on removal of $Ni^{2+}$and Co^{2+} by PMAm and PVAm, experiments were conducted at three different temperatures 303, 313, and 323 K. From Fig. 12, it was observed that the adsorption decreased with increase in temperature from 303 to 323 K, which indicated that a low temperature favors metal ion removal by PMAm and PVAm. This may be due to a tendency of metal ions to escape from the solid phase to the bulk phase with an increase in temperature of the solution. A similar observation was also reported in the study on the sorption of Pb onto modified and unmodified kaolinite clay [36].

Thermodynamic parameters, such as enthalpy (ΔH°), entropy (ΔS°), and Gibb's free energy (ΔG°) were determined by Eq. (16) [37] and (17).

$$\ln(q_e m/C_e) = \Delta S^{\circ}/R - \Delta H^{\circ}/RT \tag{16}$$

$$\Delta G^{\circ} = \Delta H^{\circ} - T\Delta S^{\circ} \tag{17}$$

where m is the adsorbent dose (g/L), C_e is the equilibrium concentration (mg/L) of the metal ion in solution and $q_e m$ is the solid-phase concentration (mg/L) at equilibrium. R is the gas constant (8.314 J/mol/K) and T is the temperature (K). ΔH°, ΔS°, and ΔG° are changes in enthalpy (J/mol), entropy (J/mol/K), and Gibb's free energy (J/mol), respectively.

The values of ΔH° and ΔS° were determined from the slope ($-\Delta H^{\circ}/R$) and the intercept ($\Delta S^{\circ}/R$) of the plots of ln ($q_e m/C_e$) vs. $1/T$. The ΔG° values were calculated using Eq. (17). The values of thermodynamic parameters are presented in Table 4. Negative values of ΔG° for the adsorption of Ni^{2+} on PVAm and Cd^{2+} on PMAm and PVAm at all three temperatures indicated that the adsorption process was feasible and spontaneous in nature. The ΔG° value was slightly positive for the adsorption of Ni^{2+} showed lower affinity of PMAm for Ni^{2+}. Negative values of ΔH°

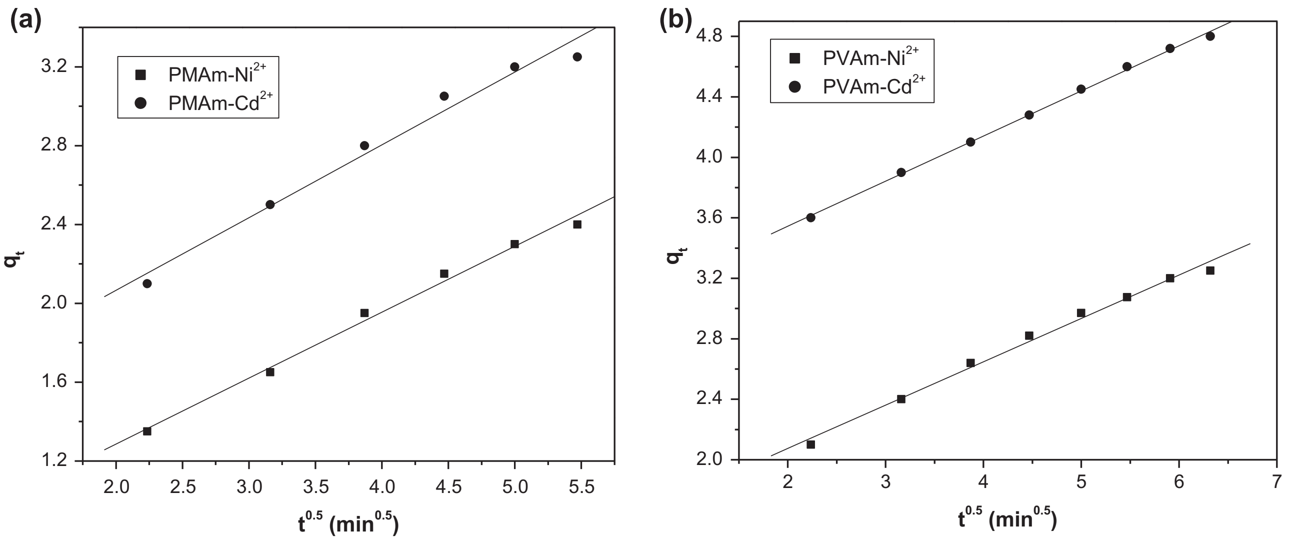

Fig. 11. Intraparticle diffusion plots for adsorption of Ni^{2+} and Cd^{2+} on PMAm (a) and PVAm (b).

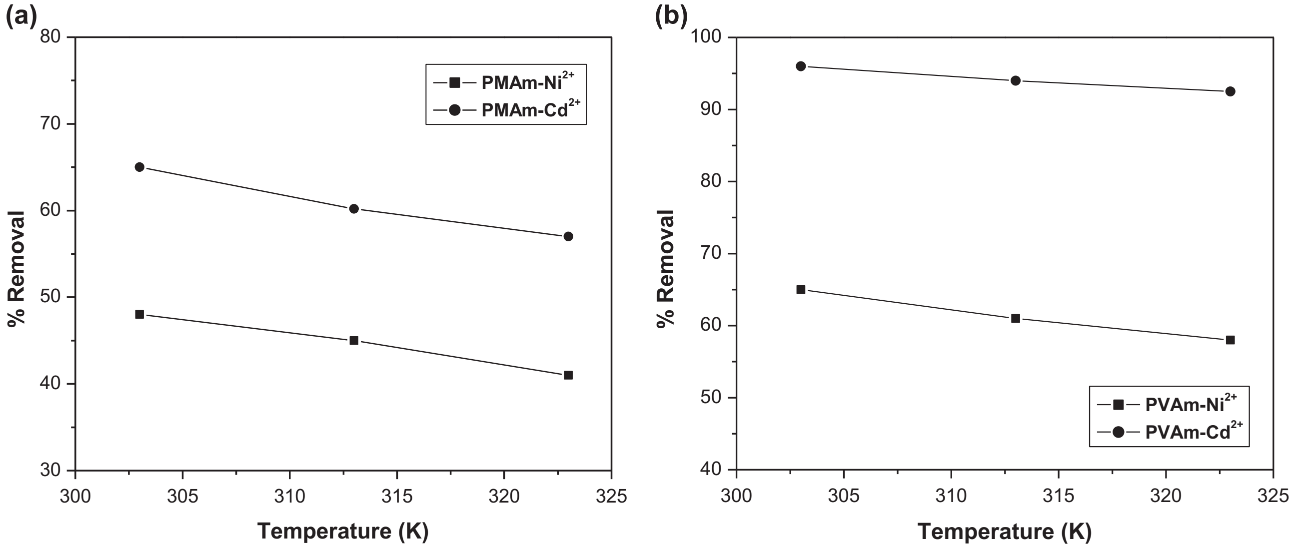

Fig. 12. Effect of temperature on removal of $Ni^{2+}$and Cd^{2+} by PMAm (a) and PVAm (b).

Table 4
Thermodynamic parameters for adsorption of Ni^{2+} and Cd^{2+} ions on PMAm and PVAm

			ΔG° (kJ/mol)		
Adsorption systems	ΔH° (kJ/mol)	ΔS° (J/mol/K)	303 K	313 K	323 K
PMAm-Ni^{2+}	−11.16	−37.44	0.179	0.553	0.928
PMAm-Cd^{2+}	−13.36	−39.01	−1.544	−1.154	−0.764
PVAm-Ni^{2+}	−11.73	−33.64	−1.545	−1.208	−0.872
PVAm-Cd^{2+}	−26.22	−60.37	−7.930	−7.327	−6.723

suggested that the adsorption process was exothermic in nature. Negative value of ΔS° described the decrease in randomness at the adsorbent–solution interface during the adsorption.

4. Conclusions

The results of the study revealed that PMAm and PVAm can be used as an effective adsorbent for the removal of Ni^{2+} and Cd^{2+} ions from various contaminated water sources. The adsorption was found to be dependent on pH, adsorbent dose, initial metal ion concentration, contact time, and temperature. The optimum pH and temperature for the adsorption was found to be 6 and 303 K, respectively. Monolayer adsorption capacity of PMAm-Ni^{2+}, PMAm-Cd^{2+}, PVAm-Ni^{2+}, and PVAm-Cd^{2+} systems was found to be 7.87 mg/g, 10.57 mg/g, 23.92 mg/g, and 31.44 mg/g, respectively. Adsorption of Ni^{2+} and Cd^{2+} on PMAm followed pseudo-first-order kinetic model and adsorption of Ni^{2+} and Cd^{2+} on PVAm followed pseudo-second-order kinetic model. Thermodynamic study revealed that the adsorption of Ni^{2+} on PVAm and Cd^{2+} on PMAm and PVAm was feasible and spontaneous in nature; however, adsorption of Ni^{2+} on PMAm showed lower affinity of PMAm for Ni^{2+}. Negative values of ΔH° suggested the adsorption process was exothermic in nature. Negative value of ΔS° described the decrease in randomness at the adsorbent-solution interface during the adsorption.

Acknowledgments

Authors are thankful to the SAIF-CDRI Lucknow for elemental analysis; Dr Dinesh Deva of Nanoscience, IIT Kanpur for recording SEM, and Council of Scientific and Industrial Research (CSIR), New Delhi, India, for the financial support.

References

[1] C.E. Borba, R. Guirardello, E.A. Silva, M.T. Veit, C.R.G. Tavares, Removal of nickel(II) ions from aqueous solution by biosorption in a fixed bed column: Experimental and theoretical breakthrough curves, Biochem. Eng. J. 30 (2006) 184–191.

[2] G.F. Nordberg, Cadmium and health in the 21st Century-historical remarks and trends for the future, BioMetals 17 (2004) 485–489.

[3] I.S. Ahmed, A.K. Ghonaim, A.A.A. Hakim, M.M. Moustafa, A.H.K. El-Din, Synthesis and characterization of some polymers for removing of some heavy metal ions of industrial wastewater, J. Appl. Sci. Res. 4 (2008) 1946–1958.

[4] C. Liu, R. Bai, Q.S. San Ly, Selective removal of copper and lead ions by diethylenetriamine-functionalized adsorbent: Behaviors and mechanisms, Water Res. 42 (2008) 1511–1522.

[5] T. Vasudevan, S. Das, S. Sodaye, A.K. Pandey, A.V.R. Reddy, Pore-functionalized polymer membranes for preconcentration of heavy metal ions, Talanta 78 (2009) 171–177.

[6] A. Nastasović, Z. Sandić, L. Suručić, D. Maksin, D. Jakovljević, A. Onjia, Kinetics of hexavalent chromium sorption on amino-functionalized macroporous glycidyl methacrylate copolymer, J. Hazard. Mater. 171 (2009) 153–159.

[7] Y.G. Zhao, H.Y. Shen, S.D. Pan, M.Q. Hu, Synthesis, characterization and properties of ethylenediamine-functionalized, Fe_3O_4 magnetic polymers for removal of Cr(VI) in wastewater, J. Hazard. Mater. 182 (2010) 295–302.

[8] G.R. Kiani, H. Sheikhloie, N. Arsalani, Heavy metal ion removal from aqueous solutions by functionalized polyacrylonitrile, Desalination 269 (2011) 266–270.

[9] E. Da'na, A. Sayari, Adsorption of copper on amine-functionalized SBA-15 prepared by co-condensation: Equilibrium properties, Chem. Eng. J. 166 (2011) 445–453.

[10] K.G. Bhattacharyya, S.S. Gupta, Kaolinite, montmorillonite and their modified derivatives as adsorbents for removal of Cu(II) from aqueous solution, Sep. Purif. Technol. 50 (2006) 388–397.

[11] G.O. El-Sayed, Removal of methylene blue and crystal violet from aqueous solutions by palm kernel fiber, Desalination 272 (2011) 225–232.

[12] K.S. Hui, C.Y.H. Chao, S.C. Kot, Removal of mixed heavy metal ions in wastewater by zeolite 4A and residual products from recycled coal fly ash, J. Hazard. Mater. 127 (2005) 89–101.

[13] V.C. Srivastava, I.D. Mall, I.M. Mishra, Equilibrium modelling of single and binary adsorption of cadmium and nickel onto bagasse fly ash, Chem. Eng. J. 117 (2006) 79–91.

[14] M.G.A. Vieira, A.F.A. Neto, M.L. Gimenes, M.G.C. da-Silva, Sorption kinetics and equilibrium for the removal of nickel ions from aqueous phase on calcined Bofe bentonite clay, J. Hazard. Mater. 177 (2010) 362–371.

[15] N. Rajic, D. Stojakovic, M. Jovanovic, N.Z. Logar, M. Mazaj, V. Kaucic, Removal of nickel(II) ions from aqueous solutions using the natural clinoptilolite and preparation of nano-NiO on the exhausted clinoptilolite, Appl. Surf. Sci. 257 (2010) 1524–1532.

[16] A. Bhatnagar, A.K. Minocha, Biosorption optimization of nickel removal from water using *Punica granatum* peel waste, Colloids Surf. B 76 (2010) 544–548.

[17] M.E. Argun, Use of clinoptilolite for the removal of nickel ions from water: Kinetics and thermodynamics, J. Hazard. Mater. 150 (2008) 587–595.

[18] M.N. Zafar, R. Nadeem, M.A. Hanif, Biosorption of nickel from protonated rice bran, J. Hazard. Mater. 143 (2007) 478–485.

[19] A. Ewecharoen, P. Thiravetyan, E. Wendel, H. Bertagnolli, Nickel adsorption by sodium polyacrylate-grafted activated carbon, J. Hazard. Mater. 171 (2009) 335–339.

[20] E. Malkoc, Y. Nuhoglu, Investigations of nickel(II) removal from aqueous solutions using tea factory waste, J. Hazard. Mater. 127 (2005) 120–128.

[21] P.S. Kumar, S. Ramalingam, S.D. Kirupha, A. Murugesan, T. Vidhyadevi, S. Sivanesan, Adsorption behavior of nickel(II) onto cashew nut shell: Equilibrium, thermodynamics, kinetics, mechanism and process design, Chem. Eng. J. 167 (2011) 122–131.

[22] I. Mobasherpour, E. Salahi, M. Pazouki, Removal of nickel (II) from aqueous solutions by using nano-crystalline calcium hydroxyapatite, J. Saudi Chem. Soc. 15 (2011) 105–112.

[23] Y.C. Sharma, Thermodynamics of removal of cadmium by adsorption on an indigenous clay, Chem. Eng. J. 145 (2008) 64–68.

[24] W. Zheng, X.M. Li, F. Wang, Q. Yang, P. Deng, G.M. Zeng, Adsorption removal of cadmium and copper from aqueous solution by areca—A food waste, J. Hazard. Mater. 157 (2008) 490–495.

[25] D. Mohan, K.P. Singh, Single- and multi-component adsorption of cadmium and zinc using activated carbon derived from bagasse—An agricultural waste, Water Res. 36 (2002) 2304–2318.

[26] Z.A. Al-Anber, M.A.D. Matouq, Batch adsorption of cadmium ions from aqueous solution by means of olive cake, J. Hazard. Mater. 151 (2008) 194–201.

[27] P.A. Amoyaw, M. Williams, X.R. Bu, The fast removal of low concentration of cadmium(II) from aqueous media by chelating polymers with salicylaldehyde units, J. Hazard. Mater. 170 (2009) 22–26.

[28] L. Dong, Z. Zhu, H. Ma, Y. Qiu, J. Zhao, Simultaneous adsorption of lead and cadmium on MnO_2-loaded resin, J. Environ. Sci. 22 (2010) 225–229.

[29] L. Semerjian, Equilibrium and kinetics of cadmium adsorption from aqueous solutions using untreated *Pinus halepensis* sawdust, J. Hazard. Mater. 173 (2010) 236–242.

[30] K.K. Singh, A.K. Singh, S.H. Hasan, Low cost bio-sorbent 'wheat bran' for the removal of cadmium from wastewater: Kinetic and equilibrium studies, Bioresour. Technol. 97 (2006) 994–1001.

[31] M.T. Uddin, M.A. Islam, S. Mahmud, M. Rukanuzzaman, Adsorptive removal of methylene blue by tea waste, J. Hazard. Mater. 164 (2009) 53–60.

[32] B.H. Hameed, D.K. Mahmoud, A.L. Ahmad, Equilibrium modeling and kinetic studies on the adsorption of basic dye by a low-cost adsorbent: Coconut (*Cocos nucifera*) bunch waste, J. Hazard. Mater. 158 (2008) 65–72.

[33] B.H. Hameed, Grass waste: A novel sorbent for the removal of basic dye from aqueous solution, J. Hazard. Mater. 166 (2009) 233–238.

[34] S. Lagergren, About the theory of so called adsorption of soluble substances, Ksver. Veterskapsakad. Handl. 24 (1898) 1–6.

[35] Y.S. Ho, G. McKay, Pseudo-second order model for sorption processes, Process Biochem. 34 (1999) 451–465.

[36] M. Jiang, Q. Wang, X. Jin, Z. Chen, Removal of Pb(II) from aqueous solution using modified and unmodified kaolinite clay, J. Hazard. Mater. 170 (2009) 332–339.

[37] B.K. Nandi, A. Goswami, M.K. Purkait, Adsorption characteristics of brilliant green dye on kaolin, J. Hazard. Mater. 161 (2009) 387–395.